A smiilar procedure readily verifies the solution for Fig. 1b, with obtuse ϕ and negative signs in Eq. (13).

Appendix B: Reduction of Analysis to Conventional Formulation

The discussion accompanying Eqs. (3 and 4) notes that, for present purposes, a deflection w can be chosen as the generalized coordinate for Eq. (2). With this substitution, and with V_E expressed as the difference between a "total" strain energy V_S and thermally induced strain energy V_t, Eq. (2) becomes

$$(\mathrm{d}/\mathrm{d}t)\,(\delta T/\delta \dot{w}) - \delta(T - V_S)\,\delta w = \delta V_t/\delta w \tag{B1}$$

This equation is compatible with the relations,

$$V_S = \frac{1}{2} EI \int_0^{\ell} (p'')^2 \mathrm{d}r \tag{B2}$$

and

$$V_t = EI \int_0^{\ell} (p'' \cdot k - \tfrac{1}{2} k^2)\,\mathrm{d}r \tag{B3}$$

At this point, two approximations are introduced. The last term of Eq. (B3) will be dropped and, in Eq. (5), the arc length constraint will be ignored. In that case, Eq. (6) is replaced by

$$p'' \doteq \begin{bmatrix} 0 \\ w' \\ 0 \end{bmatrix} \tag{B4}$$

so that Eq. (B3) reduces to

$$V_t = EI \int_0^{\ell} k_y w'' \mathrm{d}r \tag{B5}$$

where, from Eq. (11),

$$k_y = -C[\sigma_2 - (\sigma \cdot t)\,w'] \tag{B6}$$

When the inner product is formed with the arc length constraint in Eq. (5) again ignored,

$$(\sigma \cdot t) \doteq \sigma_1 - \sigma_2 w' \tag{B7}$$

and, if quadratic terms are omitted when this is combined with the preceding equation,

$$|k_y| \doteq C(\sigma_2 - \sigma_1 w') \tag{B8}$$

This is the magnitude of the steady-state thermal curvature in conventional analysis [e.g., used in Eq. (8) of Ref. 1, based on the equivalent expression in Ref. 3, or obtained by setting $\delta k/\delta t$ to zero in Ref. 4, Eq. (5)], and dynamic analyses customarily use Eq. (B1) with the approximation in (B5).

References

[1] Augusti, G., "Comment on 'Thermally Induced Vibration and Flutter of Flexible Booms,' " *Journal of Spacecraft and Rockets*, Vol. 8, Feb. 1971, pp. 202-204.

[2] Jordan, P.F., "Comment on 'Thermally Induced Vibration and Flutter of a Flexible Boom,' " *Journal of Spacecraft and Rockets*, Vol. 8, Feb. 1971, pp. 204-205.

[3] Etkin, B. and Hughes, P.C., "Explanation of the Anomalous Spin Behavior of Satellites with Long Flexible Antennae," *Journal of Spacecraft and Rockets*, Vol. 4, Sept. 1967, pp. 1139-1145.

[4] Yu, Y.Y., "Reply by Author to P.F. Jordan and G. Augusti and New Results of Two-Mode Approximation Based on a Rigorous Analysis of Thermal Bending Flutter of a Flexible Boom," *Journal of Spacecraft and Rockets*, Vol. 8, Feb. 1971, pp. 205-208.

[5] Farrell, J.L. and Newton, J.K., "Continuous and Discrete RAE Structural Models," *Journal of Spacecraft and Rockets*, Vol. 6, April 1969, pp. 414-423.

[6] Farrell, J.L., Newton, J.K., Miller, J.A., and Solomon, E.N., "Optimal Estimation of Rotation – Coupled Flexural Oscillations," *Journal of Spacecraft and Rockets*, Vol. 6, Nov. 1969, pp. 1290-1298.

Maximum Response of Missiles due to Inertial Asymmetry

Ben Zion M. Naveh* and Zeev Mittelman†

Technion – Israel Institute of Technology, Haifa, Israel

Nomenclature

c	$= L_p/I_x$
d	= diameter
I, I_x	= transversal and axial moments of inertia, respectively
i	$= \sqrt{-1}$
I_{xz}	= centrifugal moment of inertia
$K_{1,2}$	= initial amplitudes of nutational and processional modes
K_T	= trim mode
$L(p)$	$= L_p p$, damping moment in roll due to p
$M(\alpha)$	$= M_{\alpha_I}\alpha = \frac{1}{2}\rho V^2 Sd\, C_{m_{\alpha_I}}\, \alpha$, restoring moment due to α
$M(q)$	$= M_q q$, damping moment due to q
p	= roll rate
q	= complex angular yawing velocity
S	= reference area
t	= time
V	= velocity
X, Y, Z	= body axis system
α	= complex angle of attack
α_I	= angle of attack in pitch
δ_α	$= I_{xz}/(I_x - I)$
η	$= pI_x/2I$
λ	$= M_q/2I$
$\lambda_{1,2}$	$= (1 \pm \tau)$
$\phi_{1,2}$	$= \lambda_{1,2} + i\omega_{1,2}$
ϕ	= roll angle
ρ	= air density
τ	$= \eta/\omega$
ω_0	$= (-M_{\alpha_I}/I)^{1/2}$
ω	$= (\omega_0^2 + \eta^2)^{1/2}$
$\omega_{1,2}$	$= \eta(1 \pm 1/\tau)$
$(\dot{\ })$	= derivation with respect to time

Subscripts

R	= resonance
0	= at $t = 0$

I. Introduction

THE dynamic response of missiles caused by configurational or inertial asymmetry is analyzed in detail in Ref. 1, and major results are summarized in Ref. 2. It was found that for exponentially varying roll rates the maximum response occurs generally after the so-called "steady-state linear theory resonance" ($p_R = \omega_{I_R}$).

It also was found that, in the case of roll acceleration or deceleration, the maximum response associated with

Received Sept. 27, 1976; revision received May 6, 1977.

Index category: LV/M Dynamics and Control.

*Adjunct Senior Lecturer. AIAA Member.

†Graduate Student.

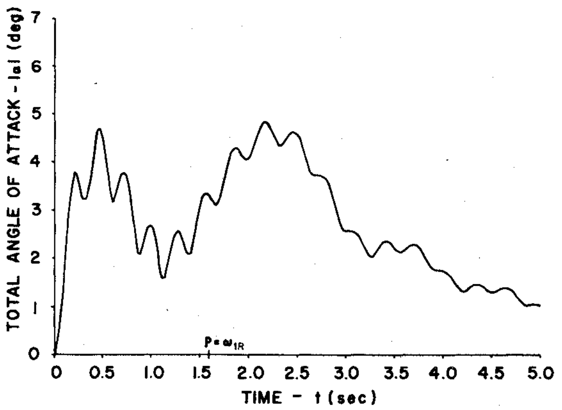

Fig. 1 Response due to inertial asymmetry, $c = -0.4$ 1/sec.

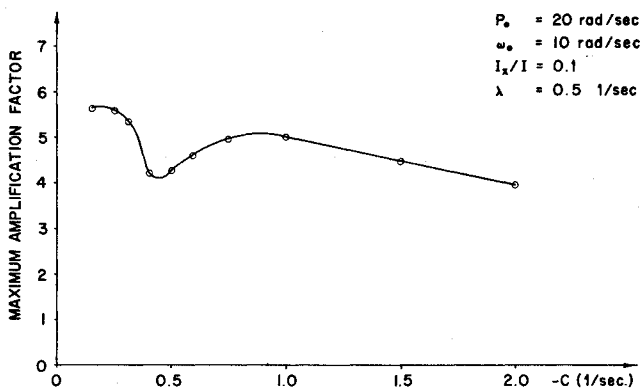

Fig. 2 Maximum amplification factor as a function of c.

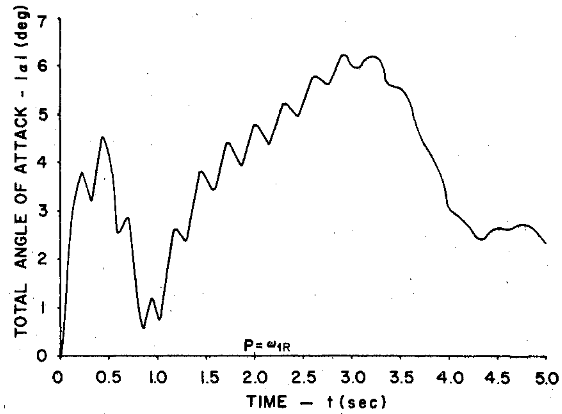

Fig. 3 Response due to inertial asymmetry, $c = -0.32$ 1/sec.

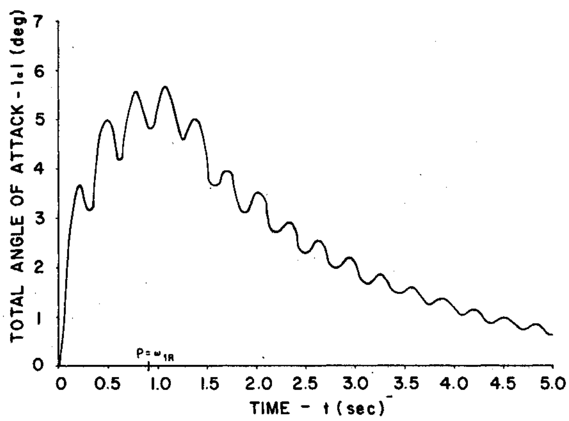

Fig. 4 Response due to inertial asymmetry, $c = -1.0$ 1/sec.

resonance is lower in magnitude in comparison to the value obtained by the steady-state linear theory. Furthermore, the maximum response decreases monotonically with roll deceleration or acceleration.[1,3]

In this paper it is shown that, in the case of inertial asymmetry and exponential roll deceleration, the maximum response associated with resonance does not decrease monotonically with roll deceleration, whereas the one caused by configurational asymmetry does decrease monotonically.[1,3]

II. Case Study

Consider the roll rate to vary exponentially and to be given by

$$p^{(t)} = p_0 e^{ct} \tag{1}$$

where

$$c = L_p / I_x \tag{2}$$

The response caused by inertial asymmetry is given by[1]

$$\alpha(t) = K_T(t) e^{i\phi} + K_1 e^{\dot{\phi}_{1R} t} + K_2 e^{\dot{\phi}_{2R} t} \tag{3}$$

where ϕ is the roll angle and

$$\dot{\phi}_{jR} = i\omega_{jR} + \lambda_{jR} \tag{4}$$

$K_T(t)$ is the third arm of the tricyclic theory, and it is calculated in detail in Ref. 1. In Ref. 2 $K_T(t)$ is given for a similar case.

While studying the response of $\alpha(t)$ for this case it was found that the maximum response associated with resonance does not decrease monotonically with roll deceleration. This result was surprising since it was found previously that, for configurational asymmetry, the maximum response associated with resonance does decrease monotonically with roll deceleration.[1,3]

Further investigations showed that, for inertial asymmetry, the maximum response due to launch conditions $[\alpha(o) = 0, \dot{\alpha}(o) = 0]$ might obtain a value that is close to the one associated with resonance, for some values of c, as shown in Fig. 1. For such cases one can notice a nonexpected drop in the value of the maximum response associated with resonance, as shown in Fig. 2.

III. Numerical Results

A special case was studied in detail using a six degrees of freedom program, where

I_x	$= 0.1$ slug-ft	(axial moment of inertia)
I	$= 1.0$ slug-ft	(transversal moment inertia)
d	$= 0.5$ ft	(diameter)
V	$= 1000$ fps	(velocity)
p_0	$= 20$ rad/sec	(initial roll rate)
δ_α	$= 1.15°$	(inertial asymmetry)
λ	$= -0.5$ 1/sec	(M_q / I yaw damping)
$C_{m_{\alpha_I}}$	$= -0.88$ 1/rad	(pitch moment coefficient)
ω_0	$= 10.0$ rad/sec	

Figure 3 shows the response for a regular case. Figure 1 shows the response for a case where the response because of launch conditions is as high as the one associated with resonance. Figure 4 shows the response for a higher value of c. The maximum response associated with resonance as a function of c is shown in Fig. 2.

References

[1] Naveh, B.Z.M., "On the Dynamic Response of Missiles with Varying Roll Rates," Ph.D. dissertation, 1975, University of Notre Dame, Department of Aerospace and Mechanical Engineering.

[2]Naveh, B.Z.M. and Brach, R.M., "On the Dynamic Response of Missiles with Varying Roll Rates," *AIAA Journal*, Vol. 14, Jan. 1976, p. 9.

[3]Murphy, C.H., "Response of a Asymmetric Missile to Spin Varying through Resonance," *AIAA Journal*, Vol. 9, Nov. 1971, pp. 2197-2201.

Heat Transfer for Highly Cooled Supersonic Turbulent Boundary Layers

William J. Cook* and Donald E. Richards†
Iowa State University, Ames, Iowa

Nomenclature

C_f = local skin-friction coefficient, $\tau_w/(\rho_e u_e^2/2)$
C_h = local Stanton number, $\dot{q}/\rho_e u_e(h_{aw}-h_w)$
h = static enthalpy
M = Mach number
M_s = Mach number of incident shock wave in shock tube
Re_v = Reynolds number, $\rho_e u_e x_v/\mu_e$
T = absolute temperature
ρu = density-velocity product
x_v = distance from virtual origin of turbulence
μ = coefficient of viscosity

Subscripts

aw = adiabatic wall
e = boundary-layer edge
m = based on measured values
p = predicted quantity
w = wall

Introduction

NUMEROUS efforts have been made to develop simple prediction schemes for skin friction and to evaluate Reynolds analogy factors $2C_h/C_f$ for turbulent supersonic and hypersonic boundary-layer flows on flat plates or equivalent zero pressure gradient surfaces. Such correlation schemes, which are useful for predicting turbulent heat transfer, are available for somewhat limited combinations of Mach number and wall cooling.[1] In this Note, a correlation of heat-transfer data is established for zero-pressure-gradient turbulent boundary layers with high wall cooling ($T_w/T_{aw}<0.3$) occurring in flows with low supersonic Mach numbers. This flow regime has not been investigated in wind tunnels and related facilities because conditions of high wall cooling at low supersonic Mach numbers cannot be produced without elaborate means of model cooling.

However, such flows can be generated in shock tubes. In shock tubes, the test Mach number M_e and the wall cooling variable h_w/h_{aw} (used in place of T_w/T_{aw} to include real gas effects) are functions of the primary shock Mach number M_s. The flows are characterized by high wall cooling and low supersonic Mach numbers. For example, in air, for the M_s range $3\leq M_s\leq 16$, $1.4\leq M_e\leq 3$ and $0.30\geq(h_w/h_{aw})\geq 0.01$. Although M_e and h_w/h_{aw} cannot be varied independently using room temperature models, h_w/h_{aw} can be varied over a wide range, whereas the corresponding range of M_e is relatively narrow.

Received Oct. 7, 1976; revision received May 19, 1977.

Index category: Boundary Layers and Convective Heat Transfer—Turbulent.

*Professor, Mechanical Engineering and Engineering Research Institute. Member AIAA.

†Graduate Assistant. Presently graduate student, Department of Mechanical Engineering, Ohio State University.

Heat-transfer measurement techniques for shock-tube flows are well known; however, techniques for skin-friction measurement in shock-tube flows are not presently available. Therefore, Reynolds analogy factors cannot be established by simultaneous measurements of heat transfer and skin friction. In view of the desirability of retaining the Reynolds analogy approach, the correlation presented here is based on predicted skin-friction values and measured heat-transfer rates.

Correlation Method

Reynolds number based on boundary-layer edge conditions and the distance from the virtual origin of turbulence is employed in the prediction of the skin friction coefficient C_f. The procedure is to transform this Reynolds number Re_v to an incompressible form $\overline{Re_v}$ by the transformation relation $\overline{Re_v}=F_x Re_v$. The corresponding $\bar{C}_f$ is next determined from an accepted $\bar{C}_f$ vs $\overline{Re_v}$ relation.[2] The compressible C_f corresponding to Re_v is then determined from the relation $\bar{C}_f=F_c C_f$. The functions F_x and F_c are unique to the prediction method. Three well-known skin-friction prediction formulations are used here: those of Sommer and Short,[3] Spalding and Chi,[4] and the Van Driest (II) method.[5] The functions F_x and F_c are presented in Ref. 1 for each of these procedures for flows in which real gas effects are not generally important.

To include the real gas effects inherent in shock-tube flows, all of the temperature ratios in the transformation functions were replaced by enthalpy ratios and $u_e^2/2h_e$ was substituted for the term $(\gamma-1)M_e^2/2$. The recovery factor was taken as 0.9 throughout. For specified flow conditions, the outlined procedure produces three predictions for C_f that do not necessarily agree. Assumption of a Reynolds analogy factor in conjunction with any of the three skin friction prediction methods would permit prediction of Stanton numbers for comparison with corresponding experimental Stanton numbers. An alternate method would be to form a Reynolds analogy factor based on the experimental Stanton number C_{hm} and the predicted skin-friction coefficient C_{fp} and then seek a correlation in terms of this Reynolds analogy factor. The latter approach is taken here. In general the Reynolds analogy factor would be expected to depend on both M_e and h_w/h_{aw}. As previously noted, M_e varies over a rather narrow range when h_w/h_{aw} is varied over a large range. Therefore, a correlation is sought between $2C_{hm}/C_{fp}$ and the wall cooling variable h_w/h_{aw}.

Previous pertinent shock-tube studies, which present heat-transfer measurements in air for the highly cooled turbulent boundary layer on a flat plate or equivalent surface, are those of Hopkins and Nerem[6] and Jones.[7] Additional experimental data were obtained in the present study and are reported in detail in Ref. 8. Table 1 shows the range of each of the studies. Primary data acquired in shock-tube testing include incident shock speed, initial pressure and temperature of the test gas, the heat flux $\dot{q}$ measured at known x positions, and the location of the virtual origin of turbulence. For the studies described in Refs. 6 and 8, x_v was taken as the location of the boundary-layer trips used to promote turbulence, and for the Jones study,[7] x_v was taken as the location of departure from laminar flow.[8] The flow variables M_e, unit Reynolds number, and h_w/h_{aw} in the test region behind the incident shock wave and can be computed with the aid of real air charts. In turn, the corresponding values of C_{fp} and C_{hm} can be computed to produce the Reynolds analogy factor $2C_{hm}/C_{fp}$.

Results and Discussion

The results obtained from analysis of the data of the three experimental studies listed in Table 1 using the Van Driest II method to predict C_f are presented in Fig. 1. A scale of edge Mach number is also shown. Although scatter exists in the results, particularly at low values of h_w/h_{aw}, the data for the three studies generally complement each other. Three data points based on Jones's study exhibit good agreement with the